Derivation and validation of a whole-body dynamic mean thermal sensation model

Marika Vellei [a,b,*]

[a] Univ. Bordeaux, CNRS, Bordeaux INP, I2M, UMR 5295, F-33400, Talence, France
[b] Arts et Metiers Institute of Technology, CNRS, Bordeaux INP, Hesam Universite, I2M, UMR 5295, F-33400, Talence, France

Keywords:
Thermal sensation
Transient
Dynamic
Exercise
Gagge's two-node

A B S T R A C T

A new model predicting the whole-body Dynamic Mean thermal sensation Vote (DMV) is described. The model is useful for evaluating transient thermal conditions but is limited to uniform ones. It is based on physiological signals (mean skin temperature and its rate of change, mean skin wittedness, and core body temperature) simulated by using Gagge's two-node thermophysiological model. It is derived from empirical data obtained through experiments conducted under 160 steady-state thermal exposures at rest, 60 transient thermal conditions at rest, and 24 static thermal conditions during exercise. An independent validation is performed against 13 transient thermal conditions during exercise. The model shows good agreement (RMSE less than 0.5) with experimental observations within the range of air temperatures between 15 and 37 °C and when activity levels are below 3 met. It performs better than the widely used Fanger's PMV model, especially when far from thermal neutrality, for step-change thermal transients, and under exercise conditions. Furthermore, the model's simplicity and low computational cost are important advantages over more complex and computationally expensive thermal sensation models based on multi-segment and multi-node thermophysiological models.

1. Introduction

As humans, we are frequently exposed to transient thermal conditions during our daily lives. These dynamic exposures can result from our actions such as changes in clothing, body posture, and activity. They can be encountered in free-running buildings due to fluctuating temperatures and air velocities, and in any building when transitioning between different thermal zones, and between the building and the outdoors. Lately, ways forward for actively implementing heating and cooling set-point temperature modulations are being explored to promote building energy savings and boost their energy flexibility as part of demand-management electricity programs [1].

Despite transient thermal states being widespread in the built environment and despite their potential to create thermal delight [2–5] and enhance building occupants' well-being [6] and health [7–9], a quantitative model to describe both dynamic thermal sensation and comfort under uniform conditions does not yet exist [10]. As a consequence, researchers and practitioners continue to use steady-state indices of thermal comfort, such as Fanger's PMV and PPD [11], even when evaluating thermal conditions characterized by rapid changes in either environmental or personal variables [12–19]. However, Fanger's model is only suited to predict thermal comfort near the zone of neutrality [20] and under steady-state or slowly changing indoor conditions [21].

To predict the dynamic physical interaction between an occupant and its environment, it is necessary to simulate the heat transfer phenomena inside the body and at its surface. This can be achieved by using thermophysiological models, which are mathematical models of human thermoregulation [22]. The predicted core body and skin temperatures can then become inputs for thermal perception models, which can be developed from regression analysis of observed thermal sensation and thermal comfort votes and simulated or monitored physiological parameters.

Several multi-segment and multi-node thermophysiological models have been developed in recent years (e.g., the JOint System Thermoregulation Model JOS-3 [23], the Human Thermal Model FIALA-FE [24], the Berkeley Comfort Model [25], and ThermoSEM [26]). These models simulate core body and skin temperatures for different regions of the human body under asymmetric environmental conditions and require coupling with equally complex predictive models of local and overall thermal sensation and comfort. The best-known of these models

Abbreviations: TSV, Thermal Sensation Vote; PMV, Fanger's Predicted Mean Vote; SMV, Static Mean Vote; DMV, Dynamic Mean Vote.

* Univ. Bordeaux, CNRS, Bordeaux INP, I2M, UMR 5295, F-33400, Talence, France.
E-mail address: marika.vellei@u-bordeaux.fr.

https://doi.org/10.1016/j.buildenv.2024.111469

is the ABC Advanced Berkeley Comfort model derived by Hui Zhang and able to predict local and overall thermal sensation and comfort for 19 body parts [2–4].

Despite its notable contribution to the understanding of thermal comfort, Zhang's model has not been largely used for simulating thermal sensation and thermal comfort in the context of the built environment. Its ability to address sensory thermal responses from 19 human body parts is of little utility in most building energy simulations, which only provide average environmental conditions for the simulated thermal zones. Moreover, the high level of insulation of new and renovated buildings leads to little asymmetry and rather homogenous temperature distributions which make multi-segment and multi-node models of little use. Another limitation is represented by the computational burden associated with their implementation, which is a practical obstacle for researchers and practitioners especially when they need to run multiple simulations.

For a wide range of design problems and applications in the context of the built environment, it is useful to develop a computationally lighter tool that can be used under uniform thermal conditions. This work specifically addresses this research gap and aims to describe, validate, and provide in open access a new analytical thermal sensation model that can predict the whole-body Dynamic Mean thermal sensation Vote (DMV) of a group of people. The model uses as inputs the mean skin temperature and its rate of change, the mean skin wittedness, and the core body temperature simulated by using the classical Gagge's two-node thermophysiological model [27]. The mean thermal sensation vote is predicted based on the widely used ASHRAE seven-point scale [28].

Few physiological-based mathematical models of dynamic thermal sensation are found in the existing literature. In a previous review [10] four main models were identified (the input parameters are shown in parenthesis).

- Zhang's ABC Advanced Berkeley Comfort model ($\Delta T_{sk,mean}$, $\Delta T_{sk,local}$, $\partial T_{sk,local}/\partial t$) [2–4];
- Fiala's Dynamic Thermal Sensation (DTS) model (ΔT_{core}, $\Delta T_{sk,mean}$, $\partial T_{sk,mean}/\partial t$) [29];
- Takada's model ($\Delta T_{sk,mean}$, $\partial T_{sk,mean}/\partial t$) [30];
- Kingma's model ($T_{sk,mean}$, $\partial T_{sk,mean}/\partial t$) [26];

Where $\Delta T_{core}/\Delta T_{sk,mean}/\Delta T_{sk,local}$ are the differences between the body core, mean skin and local skin temperatures in the actual conditions and their neutral threshold values, $\partial T_{sk,mean}/\partial t$ and $\partial T_{sk,local}/\partial t$ are the rates of change of the mean and local skin temperatures, respectively. The new DMV model is inspired by the structure of Fiala's DTS model [29] but has three specific features.

- it accounts for the impact of high relative humidity at high air temperatures by including skin wittedness as a model input;
- it better accounts for the psycho-physiological phenomenon of "thermal overshoot" as a function of both the rate of change of the mean skin temperature and the mean skin temperature;
- it explicitly takes into consideration the effect of high core body temperatures during exercise.

These specificities of the model are also not part of the ABC Advanced Berkeley Comfort model which does not consider skin wittedness, only relates the *thermal overshoot* to the rate of change of the mean skin temperature, and does not account for higher metabolic activities than sedentary.

2. Preliminary knowledge and models

2.1. Thermal sensation and thermal comfort

Humans can directly sense the temperature of the body via thermoreceptors distributed throughout its surface and within it. These thermoreceptors are expressed in *primary sensory neurons*, that convert thermal stimuli into pulses of electrical discharge, commonly described as "firing rates", which travel to *secondary sensory neurons*, where they are further processed before being transmitted to the *central nervous system* (CNS) [31,32]. While thermal perception originates in the CNS, different zones of the CNS are implicated in different dimensions of it. Thermal sensation (i.e., feeling warm, neutral, cold, etc.) is regarded as its discriminative or objective dimension; it principally depends on signals from peripheral thermoreceptors [33] and is formed in the *primary somatosensory cortex* and the *thalamus*. Thermal comfort is the affective or hedonic component of thermal perception and has been defined as "that state of mind which expresses satisfaction with the thermal environment" [28]. Thermal comfort depends on the interaction between signals from peripheral and central thermoreceptors [33] and is believed to originate in the *lateral parabrachial nucleus*. It can be assessed using different semantic constructs, for example, thermal acceptability, thermal preference and/or thermal pleasure. Thermal discomfort (and not thermal sensation) motivates thermoregulatory behaviours in humans, which have been described as "an attempt to avoid what humans call thermal discomfort or displeasure and to obtain thermal pleasure" [34]. Thermal comfort is more difficult to predict than thermal sensation because it is more strongly affected by contextual non-thermal factors. In this work, the focus is on predicting thermal sensation; another article will be dedicated to the prediction of thermal comfort from thermal sensation.

2.2. Thermal overshoot and thermal alliesthesia

Under dynamic thermal conditions, human thermal sensation can anticipate body temperature variations [35] and exaggerate the final steady-state sensory response [36]. This anticipatory and overshooting behaviour has been referred to as *thermal overshoot*. It depends primarily on the ability of sensory neurons to detect the rate of change of the skin temperature and to send this information to the CNS through spiking of their firing rates [37,38]. However, thermal overshoot is not the only psycho-physiological phenomenon affecting thermal perception during dynamic conditions. Pleasurable and unpleasurable thermal states can arise during environmental transients when whole-body thermal discomfort is suddenly removed/increased. Cabanac referred to this "property of a given stimulus to arouse pleasure or displeasure according to the internal state of the participant" with the term "thermal alliesthesia" [39]. Extant empirical evidence now shows that positive/-negative thermal alliesthesia does not only depend on the internal load error but can also be induced in the thermoneutral zone when one or more body parts are heated or cooled to reduce/increase the whole-body peripheral load error [40–42]. Thermal overshoot and thermal alliesthesia occur simultaneously during transient conditions and, therefore, are closely intertwined with one affecting the descriptive dimension of thermal perception (thermal sensation) and the other the affective one (thermal comfort) [43,44]. In this work, the focus is on modelling how the thermal overshoot affects thermal sensation during dynamic conditions, another article will be dedicated to also accounting for the phenomena of thermal alliesthesia when predicting thermal comfort from thermal sensation. For a more in-depth review of the current state of knowledge regarding thermal comfort under non-steady-state conditions, readers are referred to Ref. [10].

2.3. Effect of exercise

During exercise, a significant portion of the metabolic rate required to do external work is converted into heat which causes an increase in core body temperature. Findings indicate that even when core body temperature is elevated thermal sensation is still dominated by the mean skin temperature [45]. However, the relationship between thermal sensation and mean skin temperature when exercising is not the same as

that observed during rest since exercise reduces thermal sensitivity. This effect is much more pronounced in the cold as evidenced by human thermosensitivity studies [46–48]. The physiological mechanisms behind the reduction of thermal sensitivity are still not well understood but it can be hypothesized that the effect of a high metabolic rate and associated high core body temperature is to shift the neutral threshold for the skin temperature, for example towards lower values in the cold. This is in line with other well-documented changes in the threshold values regulating autonomic thermoregulatory responses, e.g., during the day due to the circadian clock [49], during the menstrual cycle [50–52], or due to fever [53]. For the case of fever, it is thought that pyrogens (perhaps prostaglandin E2) increase the neutral thresholds for thermoregulation, allowing the core body temperature to increase. With a similar mechanism, the synthesis and release of various substances during exercise (including prostaglandins) could cause a shift in the mean skin temperature threshold regulating cold defence responses.

2.4. Gagge's two-node model

Gagge's two-node model is a simple, lumped parameter model in which the human body (i.e., the passive/controlled system of human thermoregulation) is simulated as two concentric thermal compartments: a core cylinder (simulating muscle, subcutaneous tissue, and bone) surrounded by a thin skin outer layer (simulating the epidermis and dermis) [27,54]. The model simulates the heat transfer between the two compartments and between the outer layer and the environment. All the heat is assumed to be generated in the core compartment and the temperature within each compartment is assumed to be uniform. The active/controlling system of the model simulates the regulatory responses of vasoconstriction, vasodilatation, sweating, and shivering based on a simple linear, temperature-based control theory of human thermoregulation. The model simulates the heat exchange and the temperature change of the two body compartments at 1-min intervals. The performances of Gagge's model have been tested against experimental data for a wide range of thermal conditions [55,56] and it has been observed that.

- both core body temperature and mean skin temperature predictions are accurate in neutral conditions and reasonable in warm and hot conditions at rest,
- core body temperature predictions are poor in cool and cold environments, especially for air temperatures less than 5 °C, while mean skin temperature predictions are more accurate in such environments at rest,
- core body temperature predictions are poor in conditions of moderate to high exercise intensity (approximately from 3.5 met to 8 met) as the model underestimates the rise in core body temperature that accompanies exercise, especially in conditions with no air movement. However, mean skin temperature predictions are more accurate in such conditions.

In general, the accuracy of the model decreases as the thermal conditions become more complex with increasing levels of air movement and clothing and with exercise patterns characterized by short work and rest cycles.

2.5. Fiala's dynamic thermal sensation model

Fiala's Dynamic Thermal Sensation (DTS) model predicts the mean thermal sensation vote on the ASHRAE seven-point scale from the differences between the core body and mean skin temperatures and their neutral threshold values (ΔT_{core} *and* $\Delta T_{sk,mean}$) and the rate of change (first derivative) of the mean skin temperature $\frac{\partial T_{sk,mean}}{\partial t}$ [29]. The DTS model was developed from regression analysis of experimental data from 220 exposures to air temperatures ranging between 13 and 48 °C and activity levels between 1 and 10 met. Each experiment was re-simulated with the Human Thermal Model FIALA-FE to predict participants' mean thermophysiological responses. Statistical methods were then used to correlate the observed thermal sensation votes with the simulated physiological parameters. The threshold values for the core body and mean skin temperatures were obtained by simulating thermally neutral conditions using FIALA-FE [24].

The resulting model is composed of three main parts.

- a first part, as a function of $\Delta T_{sk,mean}$, to model the response of participants at rest under steady-state environmental conditions,
- a second part, as function of ΔT_{core} weighted by $\Delta T_{sk,mean}$, accounting for effects associated with exercise and warm core body temperatures,
- a third part, as a function of both positive and negative $\frac{\partial T_{sk,mean}}{\partial t}$, dealing with transient thermal conditions.

Fiala refers to the first and second parts as the *static comfort model*, while the third part simulates the *dynamic component* of human thermal sensation. The dynamic term depends on $\frac{\partial T_{sk,mean}}{\partial t}^{\langle - \rangle}$ to account for the thermal overshoot caused by the skin cooling down. While to account for the thermal overshoot caused by the skin warming up, the dynamic component depends on the term $e^{a \bullet t} \bullet \frac{\partial T_{sk,mean}}{\partial t}^{\langle + \rangle}_{max}$ that represents the time-weighted maximum positive rate of change of the skin temperature. This dynamic term was derived from Fiala's assumption that, during skin warming, the thermal sensation is governed by the most intense rate of change of skin temperature, weighted by a function of the time elapsed since its occurrence.

3. Methods

This section describes the methodology adopted to develop the Dynamic Mean Vote. It starts by introducing the datasets used to derive and validate the DMV model (3.1). It is then detailed how Gagge's two-node model is applied to simulate participants' thermophysiological responses (3.2). The section ends with a step-by-step description of the model's analytical derivation (3.3).

3.1. Datasets

The literature was surveyed [10] to identify laboratory experiments that provided sufficient data to derive and validate the DMV model. The following selection criteria were adopted only to include experiments.

- dealing with air exposures as water exposures are outside the domain of application of the model,
- published in peer-reviewed articles,
- where the Thermal Sensation Vote (*TSV*) was surveyed on the classical ASHRAE seven-point scale: "Hot" (+3), "Warm" (+2), "Slightly Warm" (+1), "Neutral" (0), "Slightly Cool" (−1), "Cool" (−2), and "Cold" (−3) [50].
- where the mean observed values of the air temperature T_a, mean radiant temperature T_r, relative humidity *RH*, air velocity V_a, participants' clothing insulation (in clo) and metabolic rate (in met) could be manually extracted and given as time-dependent input variables to Gagge's model.

A tabulated summary of the environmental and personal conditions studied in each experiment is given in the Supplementary File no. 1. Each experiment was simulated with Gagge's two-node model to predict participants' mean thermophysiological responses with a time step of 1 min. The clothing values given in Supplementary File no. 1 include the insulation of the chair for sitting participants. When the clothing insulation of the chair was not specified it was assumed to be equal to 0.1 clo.

This was the case for datasets no. 7, 8, 14, 17, 20, 21, 26, and 28. In all the experiments, the mean radiant temperature was approximately equal to the air temperature. The metabolic rate for sitting participants was generally set equal to 1 met. However, as can be observed in the Supplementary File no. 1, this was not the case in all the experiments as the degree of activities of participants can vary while sitting. The activity performed before the experiment can also influence the metabolic rate during the experiment if the duration of the thermal adaptation period is not sufficiently long. A sitting metabolic rate higher than 1 met was set for datasets no. 9, 10 and 11 based on the indications found in the corresponding articles.

Most of the thermal sensation data were manually retrieved using WebPlotDigitizer [57] from graphs showing the time-dependent mean responses of a group of participants. Only mean votes (and not the individual participants' votes) were used to derive and validate the model and, for this reason, the DMV only predicts the "mean" thermal sensation vote without considering any effect of interindividual variability. This limitation is further discussed in section 6.1.

A description of the two largest and most important sets of experiments included in the dataset is provided in the following two paragraphs.

3.1.1. Nevins & Rohles's experiment

A total of 1600 participants were exposed to 160 steady-state thermal exposures in groups of 10 (half females and half males) for 3-h periods [58]. Half of the participants were tested in the afternoon (14:00–17:00) and the other half in the evening (19:00–22:00). No participant was used for more than one test. The 20 tested air temperatures ranged from 15.6 to 36.7 °C with increments of 0.56 °C, thus covering the whole range of the ASHRAE seven-point scale. Eight levels of relative humidity were selected: 15, 25, 35, 45, 55, 65, 75, and 85%.

3.1.2. McNall's experiment

A total of 420 participants were exposed to three different activity levels under different steady-state thermal conditions for a total of 30 exposures [59]. Participants were tested in groups of 10 (half females and half males) for 3-h periods, with half of the participants tested in the afternoon (13:30–16:30) and the other half in the evening (18:30–21:30). No participant was used for more than one activity level. Nine to twelve combinations of air temperature and relative humidity were tested for each activity level, see Supplementary File no. 1. For the low activity level, the exercise consisted of alternating 5 min of walking with 25 min of standing; for the medium activity level, 5 min of walking were alternated with 10 min of standing, while the high activity level consisted of 5 min of walking and standing alternatively.

3.2. Thermophysiological simulations

Gagge's two-node model was originally developed in 1971 [27] and has undergone many iterations and refinements so that several versions are now available. The version of the model used in this work is mainly based on the Python code provided in version 2.8.10 (the latest at the time of writing this article) of *pythermacomfort* [60]. This version has been slightly modified to allow for minute-by-minute predictions since the model in *pythermacomfort* is coded to calculate a variety of thermal comfort indices after a simulation of 60 min.

The different existing versions of Gagge's model adopt different values for the coefficients of vasodilation C_{dil}, vasoconstriction C_{str}, and regulatory sweating C_{str} and for the neutral temperature thresholds triggering autonomic thermoregulatory responses, i.e., $T_{sk,mean,threshold}$ and $T_{core,threshold}$. Gagge himself proposed different values in different publications, further contributing to the confusion. A tabulated summary of the most often used values is given in the Supplementary File no. 2. The first set of values shown in the Supplementary File no. 2 is the one originally provided by Gagge. The second set is the last one provided by Gagge which is also the one adopted by Haslam [56] who has conducted the most extensive validation of the model so far. The third set is the one used by Doherty & Arens, 1988 [55] and Fountain & Huizenga, 1995 [61]. The fourth set is the one proposed in the ANSI/ASHRAE Standard 55 [28] and adopted by *pythermalcomfort* [60]. These coefficients and thresholds significantly affect the model's predictions. The decision taken in this work was to adopt the values proposed in the ANSI/ASHRAE Standard 55 and *pythermalcomfort* with the sole exception of C_{dil} which was set equal to the value of 50 L/(m^{2}hK) found in the 2021 ASHRAE Handbook—Fundamentals [62]. Among all the tested values for C_{dil} (i.e., 50, 75, 120, and 200 L/(m^{2}hK)) this was the one reducing the model's tendency to underestimate T_{core} during exercise and, thus, the most suitable to predict the rise in core body temperature that accompanies exercise.

Only simulated thermophysiological data were used to build the DMV model. In all simulations, Gagge's model is applied in combination with the *pythermalcomfort's* utility functions *v_relative* and *clo_dynamic* to account for modifications of the air velocity and the insulation characteristics of the clothing under exercise conditions, i.e., for metabolic rates higher than 1 met. The pre-experimental thermal adaptation time and conditions were not always specified in the articles so it was assumed that they were always equal to: $T_a = T_r = 25.5$ °C, RH = 50%, $V_a = 0.1$ m/s, 0.6 clo and 1 met (i.e., neutral conditions as predicted by Fanger's PMV model) with a duration of 30 min.

During exercise, the metabolic rate takes between 3 and 9 min to stabilize [63–65] but the met values given in Supplementary File no. 1 are discrete ones and do not consider these real dynamics. Hence, for the thermophysiological simulations a rolling mean with a moving window of 5 min was implemented on the input met values given in the Supplementary File no. 1 to reproduce more realistic metabolic variations. The window of 5 min was the one minimizing the *RMSE* between the simulated and observed met values from dataset no. 24 [64].

Some examples of the predictive performances of Gagge's two-node model in terms of mean skin temperature and core body temperature with the chosen coefficients and thresholds are shown in Fig. 1. Although Gagge's model considers the body to have "core" and "shell" temperatures, in reality, the temperature profile of the human body is continuous and the temperatures of the deep body tissues vary. The validation of the core body temperature is here based on either rectal or oesophageal temperatures (depending on the availability) which are considered to be its most representative estimate. The shell temperature is compared with the mean skin temperature which is calculated using different formulae depending on the number of skin measurement points used in the experiment. Figs. 2 and 3 show the mean skin and core body temperatures simulated by Gagge's two-node model against predictions by the Human Thermal Model FIALA-FE. The simulated conditions are those from Nevins & Rohles's experiments that are also used to derive the static part of the DMV model. For the core body temperature, only the trends can be compared as Gagge's T_{core} does not correspond exactly to Fiala's predicted hypothalamus temperature. For a more exhaustive validation of Gagge's model, the reader is referred to previous works [55,56].

3.3. Dynamic mean vote model

To derive the whole-body Dynamic Mean Vote (DMV), a modelling approach similar to Fiala's was followed and consisted of first deriving the static part of the thermal sensation model (3.3.1) and then its dynamic part (3.3.2) under conditions at rest. These two parts were then modified to account for the effect of exercise (3.3.3).

3.3.1. Static model at rest

Data from Nevins & Rohles's 3-h steady-state experiments (3.1.1) were used to derive the static model at rest. Only the mean thermal sensation votes surveyed at the end of the 3 h were considered for building the model. Regression analysis was used to model TSV as a

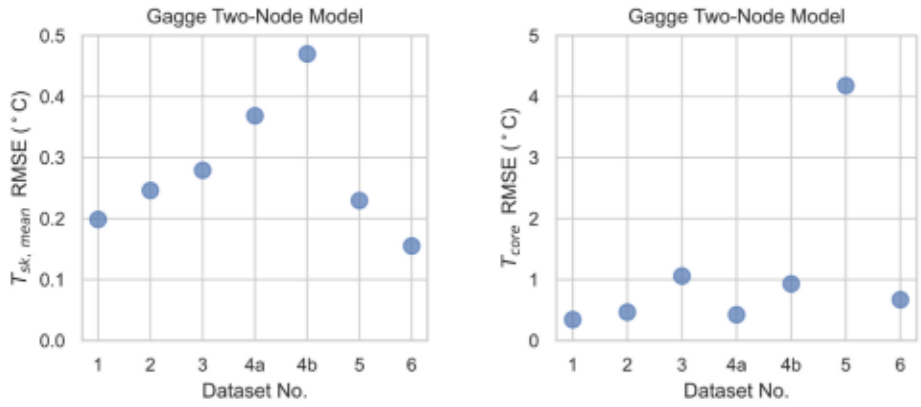

Fig. 1. Predictive performances of Gagge's two-node model in terms of mean skin (left) and core body (right) temperatures.

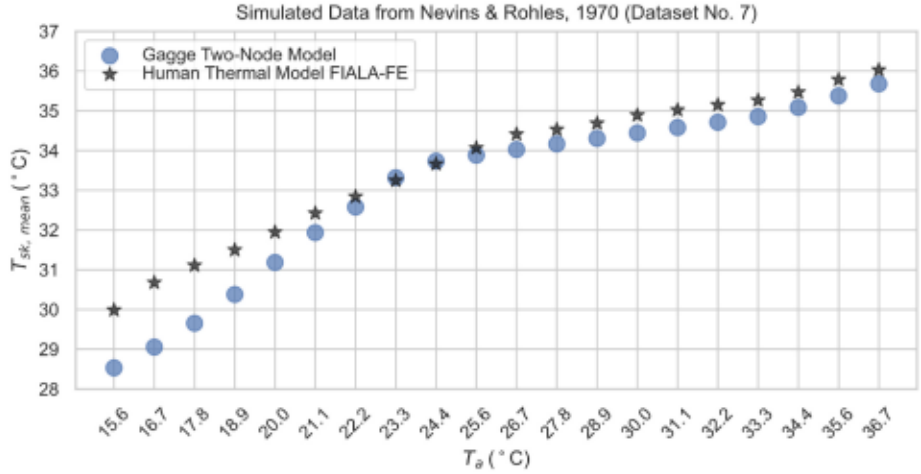

Fig. 2. Mean skin temperatures simulated by Gagge's two-node model against predictions by the Human Thermal Model FIALA-FE. The simulated conditions are those from Nevins & Rohles's experiments.

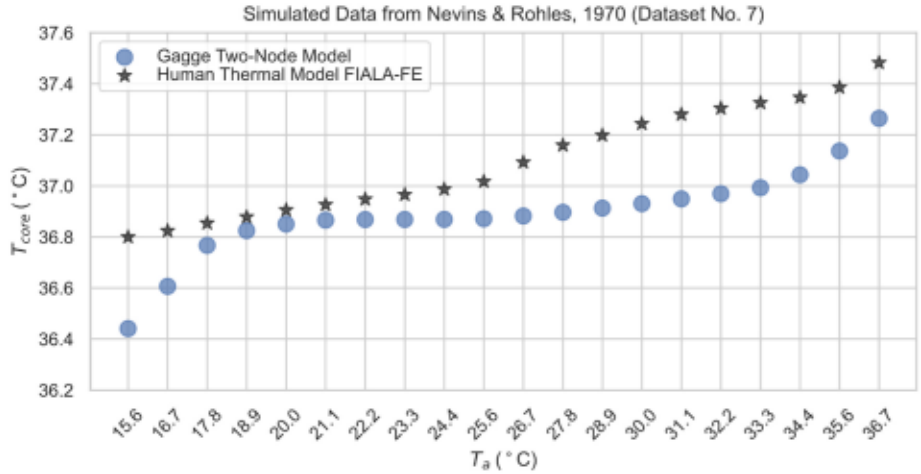

Fig. 3. Core body temperatures simulated by Gagge's two-node model against predictions by the Human Thermal Model FIALA-FE. The simulated conditions are those from Nevins & Rohles's experiments.

function of the difference between the simulated mean skin temperatures and their neutral threshold, i.e., $\Delta T_{sk,mean} = T_{sk,mean} - T_{sk,mean,threshold}$. The neutral threshold is the same as the one used in Gagge's model for triggering autonomic thermoregulatory responses, i.e., $T_{sk,mean,threshold} = 33.7°C$ (see also Supplementary File no. 2). As can be observed in Fig. 5, the thermal sensation vote does not depend linearly on $T_{sk,mean}$ but rather reaches a positive and negative asymptote at +3 and −3 when moving away from $T_{sk,mean,threshold}$ on the warm and cold side. To model this asymptotic behaviour following Fiala's approach, the hyperbolic tangent function was used, where the function's limits were extended from +1 and −1 to +3 and −3 respectively, i.e., $TSV = 3 \bullet tanh(a + b \bullet \Delta T_{sk,mean})$. Thus, $arctanh(\frac{TSV}{3})$ was the dependent

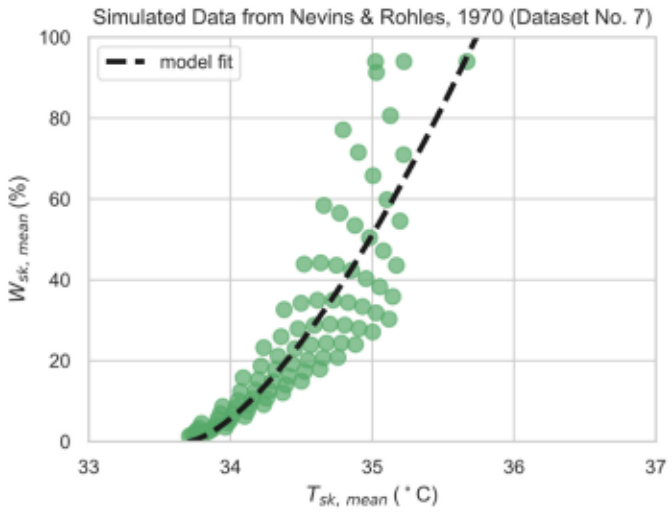

Fig. 4. Mean skin wittedness as a function of mean skin temperature. Simulated data from Nevins & Rohles, 1970.

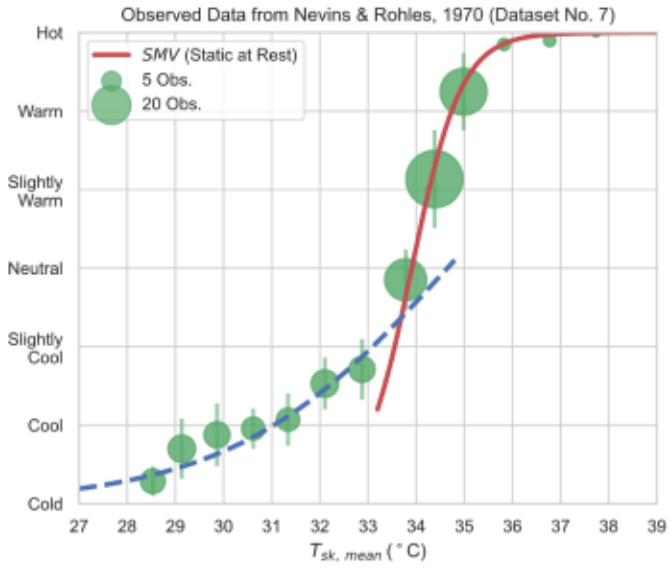

Fig. 5. Observed and simulated thermal sensation votes as a function of the simulated mean skin temperatures under steady-state thermal conditions for participants at rest. Data from Nevins & Rohles, 1970.

variable of the linear regression model, instead of TSV. Always in accordance with Fiala's method, separate models were fitted for positive ($\Delta T_{sk,mean} > 0$) and negative ($\Delta T_{sk,mean} < 0$) error signals to account for differences in thermal sensitivity to warm and cold stimuli. The key assumptions of linear regression (normality, homoscedasticity, and no autocorrelation of the residual errors) were checked and met. The Static Mean Vote at rest (*SMV*) on the cold side is then given by the following equation:

$$SMV = 3 \bullet tanh\left(a_{co} + b_{co} \bullet \Delta T_{sk,mean}\right) \quad 1$$

The coefficients a_{co} and b_{co} are defined in Table 1.

In Fiala's DTS model, the effect of mean skin wittedness is not considered. Even though humans lack a dedicated hygroreceptor, they can sense skin wittedness through the integration of cold and mechanical sensing [66]. Therefore, both contributions of mean skin temperature and skin wittedness to thermal sensation were considered in the new DMV model. This was possible since Gagge's two-node model simulates the effect of relative humidity on the evaporative heat exchange and allows the prediction of both mean skin temperature and skin wittedness. Skin wittedness $W_{sk,mean}$ is defined as the proportion of the skin covered by moisture. On the cold side ($\Delta T_{sk,mean} < 0$), Gagge's predicted mean skin wittedness is constant and equal to 0.06 so no effect of skin wittedness could be modelled. On the warm side ($\Delta T_{sk,mean} > 0$), Gagge's simulated mean skin wittedness is strongly correlated (Pearson correlation coefficient >0.8) with the mean skin temperature. Hence, to account for the effect of skin wittedness, a new variable was defined as the difference $\Delta W_{sk,mean}$ between the skin wittedness and its mean value at any given $T_{sk,mean}$ (black curve in Fig. 4) based on Nevins & Rohles's simulated data. The static thermal sensation vote on the warm side is then given by the following equations:

$$\Delta W_{sk,mean} = W_{sk,mean} - 0.06 - b_{we} \bullet \Delta T_{sk,mean}^{1.5} \quad 2$$

$$SMV = 3 \bullet tanh\left(a_{wa} + b_{wa} \bullet \Delta T_{sk,mean} + c_{wa} \bullet \Delta W_{sk,mean}\right) \quad 3$$

The coefficients b_{we}, a_{wa}, b_{wa}, and c_{wa} are defined in Table 1.

The positive value of the coefficient c_{wa} indicates that, as skin moisture levels rise, so does the perception of warmth.

The resulting static model at rest has a steeper curve on the warm side compared to the cold one as shown in Fig. 5. This indicates that humans are more sensitive to deviations in the mean skin temperature from the neutral threshold on the warm side compared to the cold side and can be explained by the fact that the mean skin temperature changes less under warm than cold thermal conditions. Indeed, from Fig. 2 it can be observed that the skin temperature decreases up to 5 °C on the cold side due to vasoconstriction while the vasodilatation-induced increase of the skin temperature on the warm side is limited to 2 °C by the evaporation of sweat.

3.3.2. *Dynamic model at rest*

The relationship between thermal sensation and mean skin temperature shown in Fig. 5 does not apply to dynamic conditions. As discussed in section 2.2 the thermal overshoot phenomenon modifies the thermal sensation during transient conditions depending on the intensity of the rate of change of the mean skin temperature.

In Fiala's modelling approach, the thermal overshoot depends on the rate of change of the mean skin temperature and its direction (warming vs cooling). It has been recently observed in rats that the detection of the warming rate is related to the inhibition of the firing rate of cold sensory

Table 1
Regression coefficients of the static thermal sensation model at rest on the cold side ($\Delta T_{sk,mean} < 0$, no. Observations: 66. Adj. R-squared: 0.594), of the model fit between ($W_{sk,mean} - 0.06$) and $\Delta T_{sk,mean}^{1.5}$ on the warm side ($0 < \Delta T_{sk,mean} < 2$, no. Observations: 90. Adj. R-squared: 0.876), and of the static thermal sensation model at rest on the warm side ($\Delta T_{sk,mean} > 0$, no. Observations: 94. Adj. R-squared: 0.814).

	Name	Coef.	Std.Err.	t	P>|t|	[0.025	0.975]
Intercept	a_{co}	−0.2116	0.074	−2.865	0.006	−0.359	−0.064
$\Delta T_{sk,mean}$	b_{co}	0.2235	0.023	9.812	0.000	0.178	0.269
$\Delta T_{sk,mean}^{1.5}$	b_{we}	0.3446	0.014	25.257	0.000	0.318	0.372
Intercept	a_{wa}	−0.2044	0.057	−3.582	0.001	−0.318	−0.091
$\Delta T_{sk,mean}$	b_{wa}	0.9747	0.053	18.560	0.000	0.870	1.079
$\Delta W_{sk,mean}$	c_{wa}	0.8034	0.256	3.135	0.002	0.294	1.312

receptors and, therefore, inherently linked with cold detection [67]. For example, the detection of a 10 °C warm step is more acute at a baseline skin temperature of 22 °C than at 32 °C [68]. Thus, in humans, the dynamic response might also depend on the absolute skin temperature in addition to the sign and magnitude of the rate of change of the skin temperature [10]. Fiala's dynamic part was developed using only two exposures to step changes in air temperature: 28-18-28 °C and 28-48-28 °C [35]. This limited set of data was not sufficient to test the above hypothesis. Hence, the dataset was extended to include longitudinal time-series experimental data collected over a wide range of dynamic conditions covering step-change, cyclical and ramp thermal transients (datasets no. 8 to 20 in Supplementary File no. 1). A modelling approach different from Fiala's was also considered and both the mean skin temperature $\Delta T_{sk,mean}$ and the rate of change of mean skin temperature $\frac{\partial T_{sk,mean}}{\partial t}$ were included in the model. The dependent variable ΔDMV was defined as the actual overshoot of thermal sensation compared to its maximum absolute possible value. For example, when the static thermal sensation is warm ($SMV = +2$) the maximum absolute change possible during skin warming is $+1$, while the maximum absolute change possible during skin cooling is $+5$. Hence, the definition of ΔDMV differs depending on the direction of the rate of change of the mean skin temperature:

$$\Delta DMV = \frac{(DMV - SMV)}{DMV_{max}} \quad where: \tag{4}$$

$$DMV_{max} = -SMV + 3 \; for \; \frac{\partial T_{sk,mean}}{\partial t} > 0 \tag{5}$$

$$DMV_{max} = SMV + 3 \; for \; \frac{\partial T_{sk,mean}}{\partial t} < 0 \tag{6}$$

By looking at the relationship between ΔDMV and $\frac{\partial T_{sk,mean}}{\partial t}$ in Fig. 6 it can be observed that ΔDMV does not grow indefinitely with $\frac{\partial T_{sk,mean}}{\partial t}$; but rather reaches a positive and negative asymptote. This asymptotic behaviour was again modelled using the hyperbolic tangent and, thus, regression analysis was applied to the linearized equation $arctanh\left(\frac{\Delta DMV}{0.55}\right) = \frac{\partial T_{sk,mean}}{\partial t} \bullet \Delta T_{sk,mean}$. The coefficient 0.55 was obtained as the result of a minimization procedure. Given the longitudinal nature of the collected time-series data, Mixed-effects Linear Models (MLM) with possible two-way interactions were employed with $\Delta T_{sk,mean}$ and $\frac{\partial T_{sk,mean}}{\partial t}$ included as fixed effects. The different experimental conditions were treated as random factors (random intercept model). The maximum likelihood was the chosen estimation method for the parameters in the MLM model. Separate models were fitted for positive ($\frac{\partial T_{sk,mean}}{\partial t} > 0$) and negative ($\frac{\partial T_{sk,mean}}{\partial t} < 0$) skin temperature transients to account for differences in the thermal sensory response to skin warming and cooling. The interaction term $\Delta T_{sk,mean} \bullet \frac{\partial T_{sk,mean}}{\partial t}$ was found to be significant only for skin warming transients. It was therefore confirmed that the skin warming-induced thermal sensation overshoot is stronger under cool compared to warm conditions. This is also evident from Fig. 6.

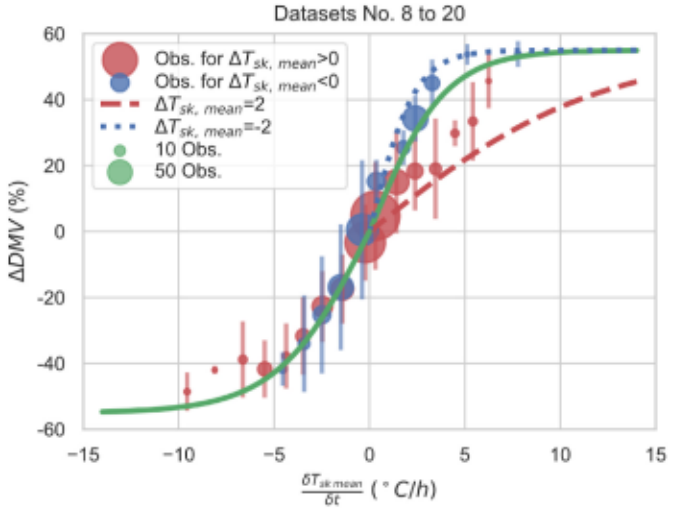

Fig. 6. Percentage dynamic change in thermal sensation as a function of the rate of change of mean skin temperature for positive and negative mean skin temperature error signals. Data are from datasets from no. 8 to 20.

The Dynamic Mean Vote for warming transients ($\frac{\partial T_{sk,mean}}{\partial t} > 0$) is then given by the following equation:

$$DMV = SMV + 0.55 \bullet tanh\left(b_{war} \bullet \frac{\partial T_{sk,mean}}{\partial t} + c_{war} \bullet \Delta T_{sk,mean} \bullet \frac{\partial T_{sk,mean}}{\partial t}\right) \bullet DMV_{max} \tag{7}$$

The coefficients b_{war} and c_{war} are defined in Table 2.

While the Dynamic Mean Vote for cooling transients ($\frac{\partial T_{sk,mean}}{\partial t} < 0$) is given by the following equation:

$$DMV = SMV + 0.55 \bullet tanh\left(b_{cool} \bullet \frac{\partial T_{sk,mean}}{\partial t}\right) \bullet DMV_{max} \tag{8}$$

The coefficient b_{cool} is defined in Table 2.

The resulting model under different dynamic conditions for participants at rest is shown in Fig. 7. Two examples of simulated and observed data from Liu et al. (dataset no. 16) are shown in Fig. 10.

3.3.3. Effect of exercise

Longitudinal time-series experimental data collected over a wide range of activity levels under static thermal conditions (datasets no. 21 to 27 in Supplementary File no. 1) were used to account for effects associated with exercise. This includes extensive data from McNall's experiments with active participants at three different activity levels (3.1.2). Only for McNall's experiment, the mean thermal sensation vote given at the end of the final standing phase was considered and the thermophysiological simulations were done with an average metabolic rate.

As discussed in section 2.3 the relationship between thermal sensation and mean skin temperature when exercising is not the same as that observed in Fig. 7 since exercise reduces thermal sensitivity, especially in the cold. A linear regression model was first applied to account for the effect of high core body temperatures under cold conditions ($\Delta T_{sk,mean} < 0$). The dependent variable was defined as the relative change in the static thermal sensation compared to its maximum possible value ΔEMV_{cold}. For example, when the static thermal sensation at rest is cold ($SMV = -2$) the maximum possible increase during exercise is $+5$. Hence, the definition of ΔEMV_{cold} is given by:

$$\Delta EMV_{cold} = \frac{(EMV - SMV)}{EMV_{max}} \quad where: \tag{9}$$

$$EMV_{max} = -SMV + 3 \; for \; \Delta T_{sk,mean} < 0 \tag{10}$$

This new variable ΔEMV_{cold} allowed to account for modifications of the static SMV due to elevated core body temperatures, similarly to the approach used for dynamic exposures. The model's independent variable was the difference between the core body temperature and its neutral threshold, *i.e.*, $\Delta T_{core} = T_{core} - T_{core,threshold}$, where the value for the threshold is the same as the one used in Gagge's model for triggering autonomic thermoregulatory responses, *i.e.*, $T_{core,threshold} = 36.8°C$ (see also Supplementary File no. 2). Given the longitudinal nature of the collected time-series data, a Mixed-effects Linear Model (MLM) was employed. The resulting model was $\Delta EMV_{cold} = a_{exe} + b_{exe} \bullet \Delta T_{core}$. In this approach, it was assumed that when exercising under cold conditions humans lose their ability to detect dynamic variations of the mean skin temperature. The thermal sensation vote during exercise on the cold side ($\Delta T_{sk,mean} < 0$) is then given by the following equation:

Table 2

Regression coefficients of the dynamic thermal sensation model at rest for warming transients ($\frac{\partial T_{sk,mean}}{\partial t} > 0$, no. Observations: 412. no. Groups: 55) and for cooling transients ($\frac{\partial T_{sk,mean}}{\partial t} < 0$, no. Observations: 433. no. Groups: 53).

	Name	Coef.	Std.Err.	z	P>|z|	[0.025	0.975]
$\frac{\partial T_{sk,mean}}{\partial t}$	b_{war}	0.255	0.012	21.749	0.000	0.232	0.278
$\Delta T_{sk,mean}$	–	−0.068	0.061	−1.105	0.269	−0.188	0.052
$\Delta T_{sk,mean} \bullet \frac{\partial T_{sk,mean}}{\partial t}$	c_{war}	−0.086	0.023	−3.796	0.000	−0.130	−0.041
$\frac{\partial T_{sk,mean}}{\partial t}$	b_{cool}	0.208	0.010	21.031	0.000	0.189	0.228

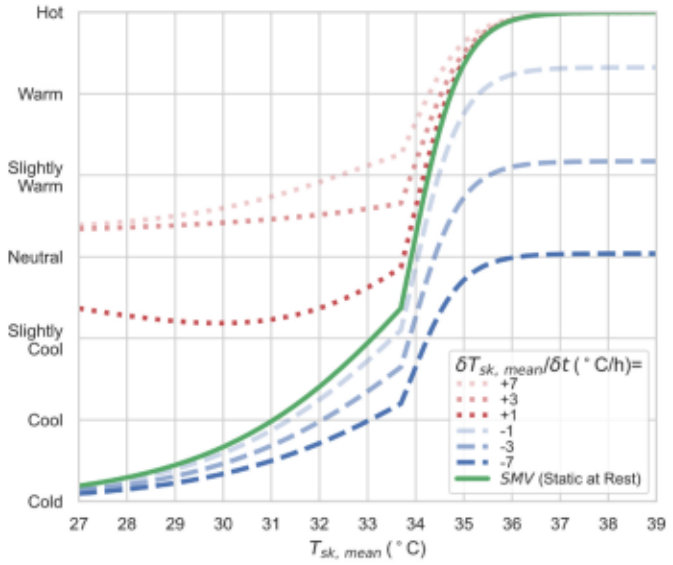

Fig. 7. Thermal sensation vote as a function of the mean skin temperature under different dynamic conditions for participants at rest.

$$EMV_{cold} = SMV + (a_{exe} + b_{exe} \bullet \Delta T_{core}) \bullet EMV_{max} \text{ for } \Delta T_{core} > 0.15 \quad 11$$

The coefficients a_{exe} and b_{exe} are defined in Table 3. The resulting model is shown in Figs. 8 and 9 for different values of ΔT_{core}.

On the warm side, the thermal sensation vote is also modified during exercise but in a much less substantial way compared to cold conditions as can be observed in Fig. 9. The dynamic component of thermal sensation also appears to be preserved so it was decided to calculate the relative change in thermal sensation compared to its dynamic value $\Delta EMV_{warm} = \frac{\langle TSV - DMV \rangle}{(DMV+3)}$ and regress it against ΔT_{core}. This regression was not significant as the relative decrease was constant and equal to 0.05 (i.e., $\Delta EMV_{warm} = 0.05$ for $\Delta T_{core} > 0.3$) as shown in Fig. 8. The resulting model was $\Delta EMV_{cold} = c_{exe}$. The thermal sensation vote during exercise on the warm side ($\Delta T_{sk,mean} > 0$) is then given by the following equation:

$$EMV_{warm} = 3 \bullet c_{exe} + (1 + c_{exe}) \bullet DMV \text{ for } \Delta T_{core} > 0.3 \quad 12$$

The coefficient c_{exe} is equal to 0.05.

Given that core body and mean skin temperatures are strongly correlated (Pearson correlation coefficient >0.8) the result would have been similar if ΔEMV_{warm} was regressed against $\Delta T_{sk,mean}$.

Two examples of simulated and observed data from Zhai et al. (dataset no. 28) are shown in Fig. 10.

Table 3

Regression coefficients of the thermal sensation model during exercise on the cold side. The dependent variable is *DTSV*. no. Observations: 210. no. Groups: 37.

	Name	Coef.	Std.Err.	z	P>|z|	[0.025	0.975]
Intercept	a_{exe}	0.087	0.024	3.562	0.000	0.039	0.134
ΔT_{core}	b_{exe}	0.768	0.032	23.721	0.000	0.705	0.831

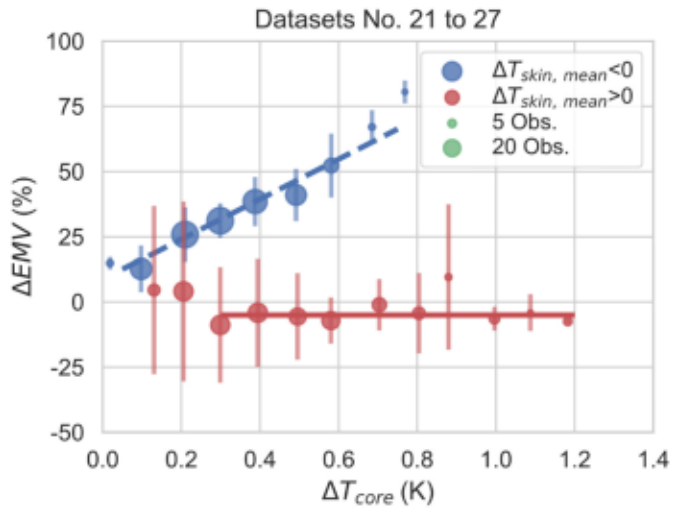

Fig. 8. Percentage change in thermal sensation as a function the difference between the core body temperatures and their neutral threshold value. Data are from datasets from no. 21 to 27.

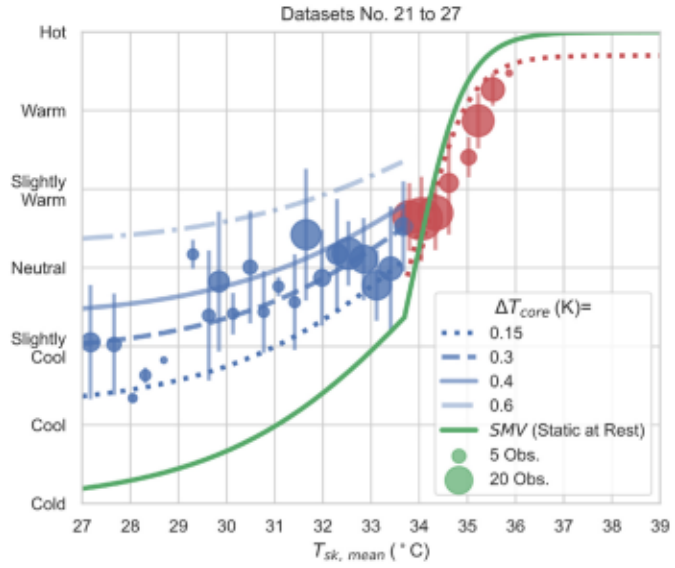

Fig. 9. Thermal sensation vote as a function of the mean skin temperature for participants under different exercise conditions characterized by different values of ΔT_{core}. Data are from datasets from no. 21 to 27.

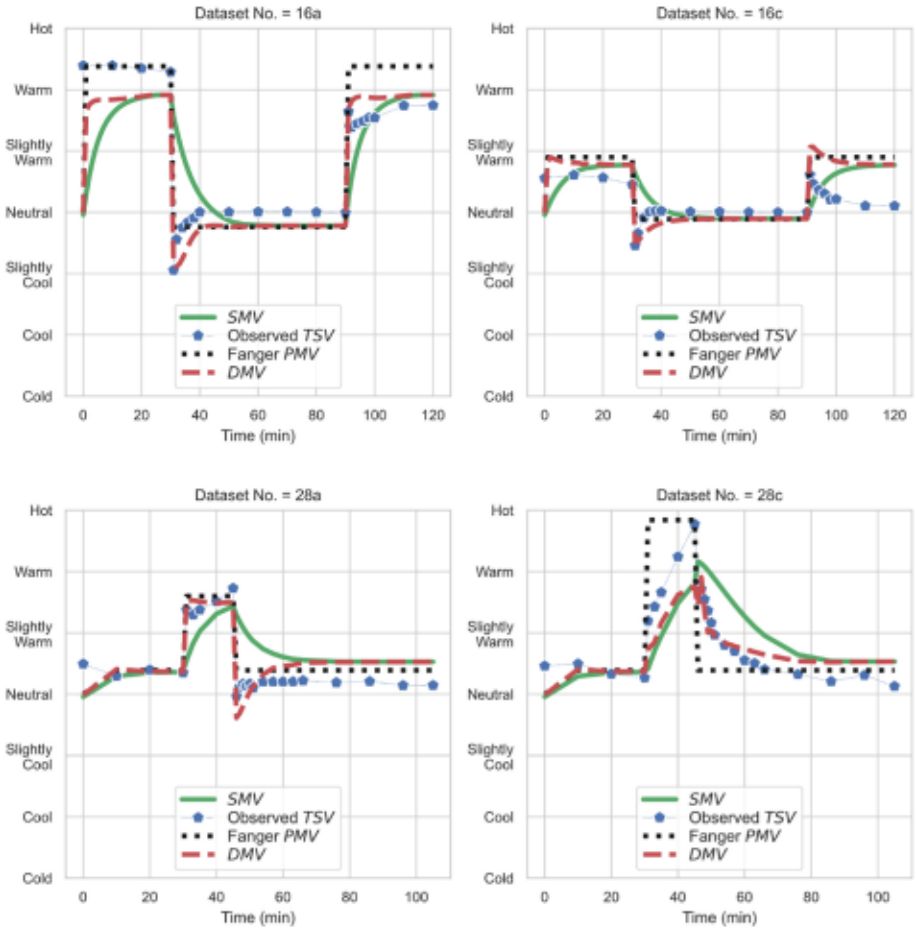

Fig. 10. Simulated and observed data from Liu et al., 2014 (dataset no. 16) and Zhai et al., 2019 (dataset no. 28).

4. Results

In this section, an overview of the predictive performances of the new DMV model against those of the widely used Fanger's PMV model [11] is reported. Fanger's PMV model is the most known and applied index in the thermal comfort literature. It is often used outside the boundaries of applicability originally defined by Fanger. Therefore, it is important to evaluate Fanger's model over all the experimental conditions reported in section 3.1 covering both steady-state and transient environmental conditions and spanning a range of different exercise intensities.

The root-mean-square-error (*RMSE*), the mean absolute error (*MAE*) and the *bias* were used to measure and compare the difference between the observed and predicted indices.

$$RMSE = \sqrt{\frac{\sum (OV - PV)^2}{n}} \quad 13$$

$$MAE = \frac{\sum |OV - PV|}{n} \quad 14$$

$$bias = \frac{\sum (OV - PV)}{n} \quad 15$$

where OV is the observed value, PV is the predicted value, and n is the number of data points. The *RMSE*, *MAE* and *bias* were always calculated over the course of the experimental conditions but it was decided to exclude the first 30 min of the exposure as there was always uncertainties over the participants' exact initial thermal conditions. Overall mean predictive performance in terms of *RMSE*, *MAE* and *bias* of the new DMV model against those of Fanger's PMV index are summarized in Table 4.

In a prior extensive validation study [21], the accuracy of thermal sensation predictions was regarded as acceptable when the RMSE was within 1 unit, a value consistent with the typical standard deviation of thermal sensation data [69]. In this work, the same criterion was used to judge *acceptable* predictions (dashed red lines in Fig. 11, Fig. 13, Fig. 14, and Fig. 15), while *good* predictions were considered for RMSE within 0.5 units.

Fig. 11 starts by showing the RMSE on TSV for DMV against Fanger's PMV under the different air temperature conditions studied in Nevins & Rohles, 1970. It is to be highlighted that Fanger's PMV was also derived from the same data. The DMV model has consistently good predictive performances over the wide range of considered air temperatures in contrast to Fanger's PMV model whose RMSE increases when deviating further from neutrality. This predictive behaviour is further analysed in Fig. 12 which shows the mean *bias* against bins of Fanger's PMV in accordance with the validation method proposed by Humphreys and Nicol [69] and re-adopted by Cheung et al. [20]. The following binning criteria were used: $Cold < -2.5$, $-2.5 \leq Cool < -1.5$, $-1.5 \leq Slightly\ Cool < -0.5$, $-0.5 \leq Neutral \leq 0.5$, $0.5 < Slightly\ Warm \leq 1.5$, $1.5 < Warm \leq 2.5$, $Hot > 2.5$. Humphreys and Nicol deemed the PMV model unbiased when the mean *bias* fell within the range of ± 0.25, as denoted by the dashed red lines in Fig. 12. According to this criterion and based on Cheung's and Humphreys and Nicol's analysis of extensive observational data, the PMV was found to be valid only for neutral thermal conditions, while for the other six categories, including slightly warm and slightly cool, it was found not valid. Here, based on experimental data from Nevins & Rohles it is observed that the PMV performs poorly

Table 4
Summary mean *RMSE*, *MAE* and *bias* of DMV against Fanger's PMV for different thermal scenarios.

	Static		Cyclical/Ramp		Step-Change		Static Exercise		Dynamic Exercise	
	DMV	PMV	DMV	PMV	DMV	PMV	DMV	PMV	DMV	PMV
RMSE	0.37	0.74	0.36	0.36	0.33	0.44	0.56	1.97	0.58	1.03
Bias	0.00	0.08	−0.15	−0.05	0.06	0.02	0.07	−0.47	−0.25	−0.38
MAE	0.29	0.57	0.31	0.29	0.27	0.36	0.44	1.36	0.42	0.70

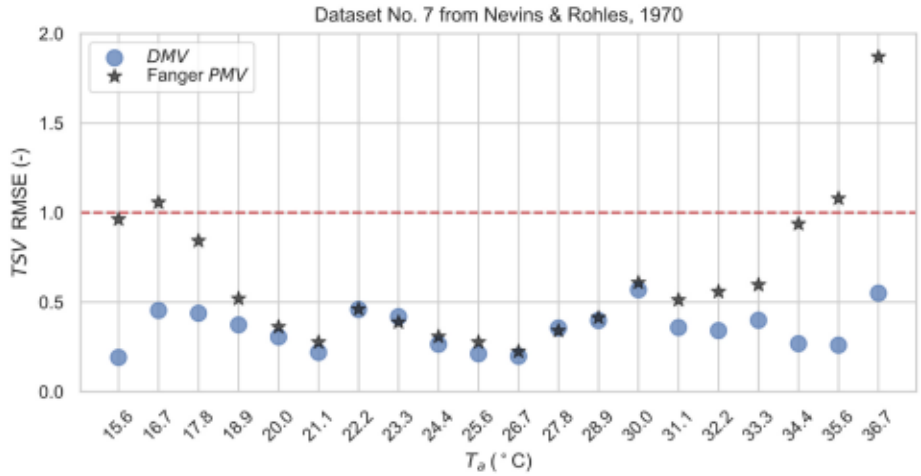

Fig. 11. RMSE on TSV of DMV against Fanger's PMV for the different air temperature conditions studied in Nevins & Rohles, 1970.

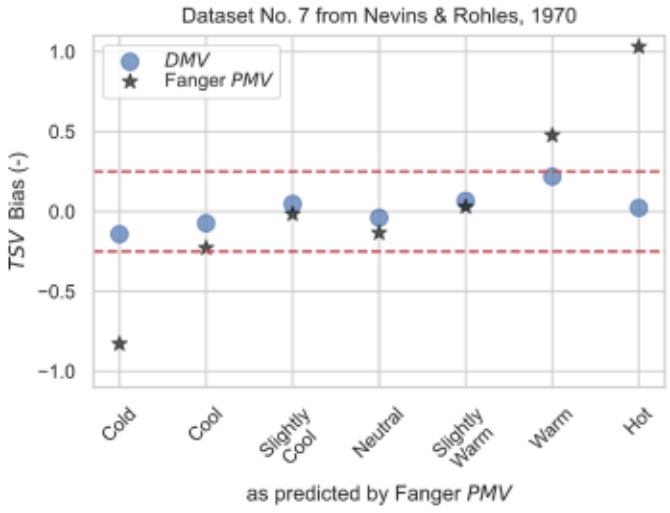

Fig. 12. Mean bias on TSV of DMV against Fanger's PMV at different bins of Fanger's PMV. Data from Nevins & Rohles, 1970.

at cold, warm and hot sensations, while its performances are good between slightly cool and slightly warm votes. The new DMV model has good predictive performances over the whole range of thermal sensations. It is to be highlighted that the predictive performances of the models shown in this section are strongly dependent on the fact that the data comes from experimental well-controlled thermal conditions. Heterogeneities and uncertainties in measuring the input parameters in the field will surely lead to poorer predictive performances.

Fig. 13 shows the RMSE on TSV for DMV against Fanger's PMV under various transient conditions. Under step-change transients, the DMV has better performances than Fanger's PMV model: the overall RMSE on TSV is equal to 0.44 for Fanger's PMV and 0.33 for the new DMV model, see Table 4. Fig. 14 shows the RMSE on TSV for DMV against Fanger's PMV for various exercise intensities under static thermal conditions. Finally, an independent validation of the new DMV model was performed against 13 complex transient thermal conditions during exercise (datasets 28, 29, and 30). Fig. 15 shows the results of the independent validation. Under exercise conditions, the DMV has consistently better performances than Fanger's PMV model: the overall RMSE on TSV is equal to 1.97 for Fanger's PMV and 0.56 for the new DMV model under static exercise. While under dynamic exercise the overall RMSE on TSV is equal to 1.03 for Fanger's PMV and to 0.58 for the new DMV model, see Table 4. However, it can be observed that the DMV's accuracy decreases as the exercise intensity increases, especially beyond 3 met (Condition no. 24b, 26f, 30d, 30g, and 30h) and under cold conditions (dataset 23 T_a = 12.2 °C). This is related to the fact that Gagge's core body temperature predictions are poor in cool and cold environments (especially for air temperatures less than 5 °C) and under exercise conditions as the model underestimates the rise in core body temperature that accompanies exercise as already highlighted in section 2.4. It is to be noted that the maximum level of exercise in the dataset is equal to 4.6 met. So, there is no information regarding the predictive performances for exercise conditions above 5 met.

5. Discussion

The DMV model, akin to any other model, is wrong. Some of the model's limitations are highlighted in the next section. However, given the high model interpretability, it can serve as a useful tool for enhancing researchers' and practitioners' comprehension and simulation of the human thermal sensory response to dynamic and exercise conditions in both indoor and outdoor settings. Here, some specificities of this new model are discussed.

The model is derived from a dataset that has been put together directly by the Author of this paper by mainly manually collecting data from published literature. While the Author has been the only one involved in this task and has taken great care, errors are unavoidable in this manual process. An estimation of the accuracy achieved has not been carried out but it is believed that this would not greatly affect the analytical from of the model and its performances shown in Table 4 as

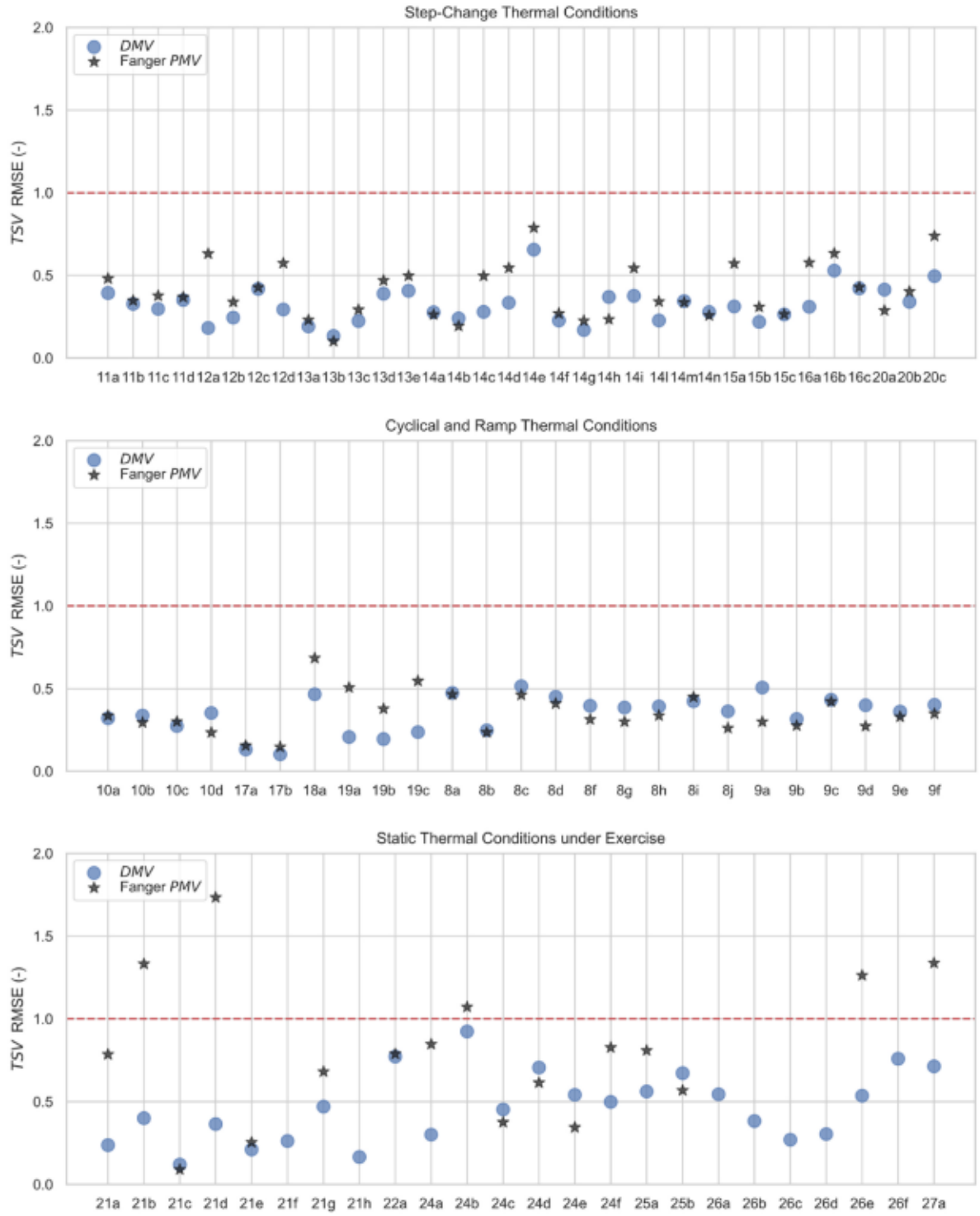

Fig. 13. RMSE on TSV of DMV against Fanger's PMV for step-change, cyclical and ramp thermal conditions and under exercise.

the database is relatively large. The need of time-series experimental thermal comfort data to develop mathematical models such as the DMV model and the current difficulties in accessing this type of data (as evidenced by the manual recovering done in this work) highlights the importance of making experimental thermal comfort data FAIR (Findable, Accessible, Interoperable, and Reusable).

The structure and predictive performances of the DMV model are inherently linked to those of Gagge's two-node model. There are several other two-node thermophysiological models in the literature. Gagge's model was here used because this model has been extensively validated as illustrated in section 2.4 so that there is an understanding of where and why it fails. Numerous variations and adaptations of Gagge's two-node model can also be found in the literature. Hence, there likely exists an improved version of Gagge's two-node model compared to the one currently implemented in *pythermalcomfort*, the version adopted for this work. The decision to use the version currently available *in pythermalcomfort* (except for the adapted coefficient of vasodilation) was dictated by the importance that this package has gained over the last years and the growing number of researchers and practitioners now using it.

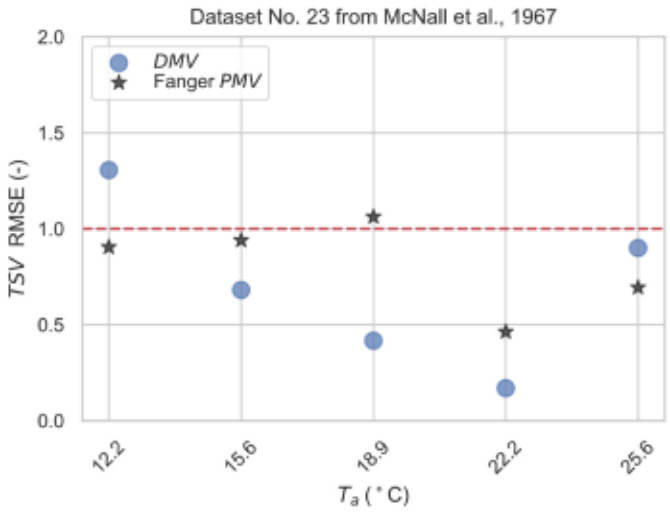

Fig. 14. RMSE on TSV of DMV against Fanger's PMV for the different air temperature conditions studied in McNall et al., 1967.

6. Limitations and future perspectives

Some major limitations of the DMV model and future perspectives for improvement are highlighted in the following paragraphs.

6.1. Effect of interindividual variability

The DMV model and the related Gagge's two-node model simulate the average thermal sensation of an average man who weighs 70 kg and has a surface area of 1.8 m^2 without accounting for any interindividual variability. While simulating the average thermal perception is useful for understanding the processes governing the dynamic sensory response, effective design solutions can be only explored when interindividual variability is considered. Interindividual variability in thermal perception originates from a diversity of physiological, psychological, and behavioural factors. From a physiological ground, several morphological and functional differences affect thermoregulation and body temperature distribution. For example, in the case of sex differences, females have on average a higher surface-to-volume ratio, higher fat mass, less muscle mass, lower body surface area, and lower metabolic rate than men [70–72]. Other than sex, individual differences can also be due to age, body build, fitness level, and geographic/ethnic acclimatization. Gagge's model is capable of addressing some physiological differences between individuals by adjusting its model inputs, for example by adapting the basal metabolic heat production for body weight and body type and the blood flow amount for body type [73]. Recent results suggest that some interindividual differences need to be considered not only in the thermophysiological model but also at the level of the thermal perception model since the relationship between thermal sensation and skin/core body temperature also varies for different individual characteristics [74]. Hence, future efforts should be dedicated to investigating and incorporating the effect of interindividual variability at both levels of Gagge's and DMV models.

6.2. Effect of intraindividual variability

Intraindividual variability is due to differences in thermal sensory responses that the same person can experience, for example, during different seasons due to thermal adaptation [75] and/or acclimatization [76,77], during the day due to the circadian clock [49], during the menstrual cycle [50–52], or due to fever [53]. The new DMV model does not account for any of these effects. Hence, future efforts should be dedicated to investigating and incorporating the effect of intraindividual variability at both levels of Gagge's and DMV models.

6.3. Effect of thermal habituation

Other than thermal overshoot and thermal alliesthesia, dynamic thermal perception is also affected by the phenomena of thermal habituation. Thermal habituation is a short-term (*i.e.*, of the order of minutes or hours) adaptive process that modifies the body's sensory response after prolonged non-neutral thermal exposures [10]. In particular, the mean skin temperatures have been observed to stabilize at slightly higher-than-neutral values after warm exposures, and slightly lower-than-neutral values after cool exposure [74,78–80]. The corresponding thermal sensations appear to be shifted in the opposite direction to the preceding thermal sensation, e.g., nudged towards slightly warm after transitioning from cool conditions. The phenomenon of thermal habitation is not included in the DMV model because Gagge's model cannot simulate this phenomenon. Future efforts should be dedicated to elucidating the psycho-physiology behind this phenomenon and to understand whether it is important enough to warrant future inclusion in the model.

6.4. Dynamics below 1 min

The DMV model has not been applied for time steps lower than 1 min so nothing can be said about the predictive performances of the model for thermal sensation simulations under 1 min. It is nevertheless important that future developments of the model explore this time dimension since some specific dynamics such as those induced by outdoor wind gusts can only be correctly modelled if time steps lower than 1 min are considered. A numerical model of cutaneous thermoreceptors might be the best approach for such a case [26,81].

7. Conclusions

In this work, a new model predicting the whole-body Dynamic Mean

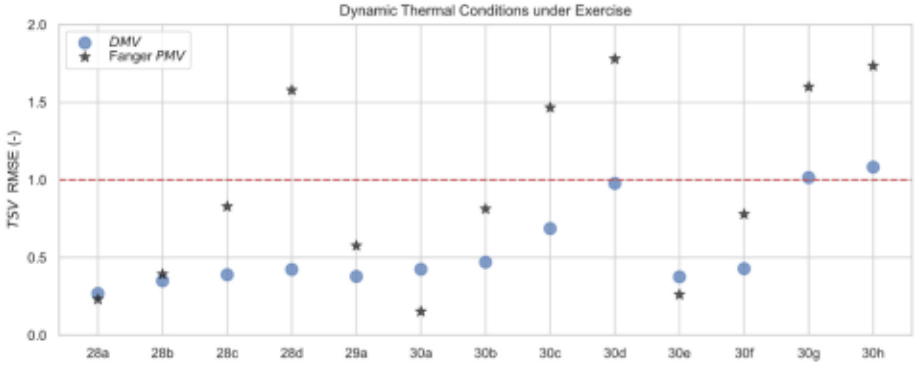

Fig. 15. RMSE on TSV of DMV against Fanger's PMV for different dynamic thermal conditions under exercise.

thermal sensation Vote (DMV) is outlined. The foundation of the model lies in physiological variables (mean skin temperature and its rate of change, mean skin wittedness, and core body temperature), simulated by using Gagge's two-node thermophysiological model. The model's formulation is based on 160 static thermal exposures at rest, 60 transient thermal conditions at rest, and 24 static thermal scenarios during exercise. The model has three novel specific features.

- It accounts for the impact of high relative humidity at high air temperatures by including skin wittedness as a model input.
- It models the dynamic sensory phenomena of thermal overshoot as a function of both the rate of change of the mean skin temperature and the mean skin temperature.
- It explicitly accounts for the effect of high core body temperatures during exercise.

Given the high model interpretability, the DMV model can serve as a useful tool for enhancing researchers' and practitioners' comprehension and simulation of the human thermal sensory response to dynamic and exercise conditions. The model's applicability is limited to uniform conditions. An independent validation is performed against 13 complex transient thermal conditions during exercise. The validation shows that the DMV model has better predictive performances than the widely used Fanger's PMV/PPD model, especially for dynamic conditions far from neutrality and under exercise.

CRediT authorship contribution statement

Marika Vellei: Writing – review & editing, Writing – original draft, Visualization, Validation, Software, Resources, Project administration, Methodology, Investigation, Funding acquisition, Formal analysis, Data curation, Conceptualization.

Declaration of competing interest

The authors declare that they have no known competing financial interests or personal relationships that could have appeared to influence the work reported in this paper.

Data availability

The data and Python codes can be accessed at 10.6084/m9.figshare.24832857.

Acknowledgements

This project has received funding from the European Union's Horizon 2020 research and innovation programme under the Marie Skłodowska-Curie grant agreement No 884556.

Appendix A. Supplementary data

Supplementary data to this article can be found online at https://doi.org/10.1016/j.buildenv.2024.111469.

References

[1] IEA Perspectives for the Clean Energy Transition - the Critical Role of Buildings, 2019.
[2] H. Zhang, E. Arens, C. Huizenga, T. Han, Thermal sensation and comfort models for non-uniform and transient environments: Part I: local sensation of individual body parts, Build. Environ. 45 (2010) 380–388, https://doi.org/10.1016/j.buildenv.2009.06.018.
[3] H. Zhang, E. Arens, C. Huizenga, T. Han, Thermal sensation and comfort models for non-uniform and transient environments, part II: local comfort of individual body parts, Build. Environ. 45 (2010) 389–398, https://doi.org/10.1016/j.buildenv.2009.06.015.
[4] H. Zhang, E. Arens, C. Huizenga, T. Han, Thermal sensation and comfort models for non-uniform and transient environments, part III: whole-body sensation and comfort, Build. Environ. 45 (2010) 399–410, https://doi.org/10.1016/j.buildenv.2009.06.020.
[5] R. de Dear, Revisiting an old hypothesis of human thermal perception: alliesthesia, Build. Res. Inf. 39 (2011) 108–117, https://doi.org/10.1080/09613218.2011.552269.
[6] J. Soderlund, P. Newman, Biophilic architecture: a review of the rationale and outcomes, AIMS Environ.Sci. 2 (2015) 950–969, https://doi.org/10.3934/environsci.2015.4.950.
[7] W. van Marken Lichtenbelt, M. Hanssen, H. Pallubinsky, B. Kingma, L. Schellen, Healthy excursions outside the thermal comfort zone, Build. Res. Inf. 45 (2017) 819–827, https://doi.org/10.1080/09613218.2017.1307647.
[8] Y.M. Ivanova, H. Pallubinsky, R. Kramer, W. van Marken Lichtenbelt, The influence of a moderate temperature drift on thermal physiology and perception, Physiol. Behav. 229 (2021) 113257, https://doi.org/10.1016/j.physbeh.2020.113257, 113257.
[9] W. Luo, R. Kramer, Y. Kort, P. Rense, W. Marken Lichtenbelt, The effects of a novel personal comfort system on thermal comfort, physiology and perceived indoor environmental quality, and its health implications - Stimulating human thermoregulation without compromising thermal comfort, Indoor Air (2021), https://doi.org/10.1111/ina.12951.
[10] M. Vellei, R. de Dear, C. Inard, O. Jay, Dynamic thermal perception: a review and agenda for future experimental research, Build. Environ. 205 (2021) 108269, https://doi.org/10.1016/j.buildenv.2021.108269, 108269.
[11] P.O. Fanger, Thermal Comfort: Analysis and Applications in Environmental Engineering, McGraw-Hill, 1972.
[12] D. Da Silva, Analyse de la flexibilité des usages électriques résidentiels : application aux usages thermiques, 2011.
[13] M.-A. Leduc, A. Daoud, C. Le Bel, Developing winter residential demand response strategies for electric space heating, in: Sydney (AU), 2011.
[14] P. Morales-Valdés, A. Flores-Tlacuahuac, V.M. Zavala, Analyzing the effects of comfort relaxation on energy demand flexibility of buildings: a multiobjective optimization approach, Energy Build. 85 (2014) 416–426, https://doi.org/10.1016/j.enbuild.2014.09.040.
[15] G. Masy, E. Georges, C. Verhelst, V. Lemort, P. André, Smart grid energy flexible buildings through the use of heat pumps and building thermal mass as energy storage in the Belgian context, Sci. Technol.for the Built. Environ. 21 (2015) 800–811, https://doi.org/10.1080/23744731.2015.1035590.
[16] J. Le Dréau, P. Heiselberg, Energy flexibility of residential buildings using short term heat storage in the thermal mass, Energy 111 (2016) 991–1002, https://doi.org/10.1016/j.energy.2016.05.076.
[17] S. Agapoff, M. Jandon, T. Guiot, Impact of a Tariff Based Heating Load Control on Energy, Comfort and Environment : a Parametric Study in Residential and Office Buildings, 2017. Leeds (UK).
[18] T.Q. Péan, J. Ortiz, J. Salom, Impact of demand-side management on thermal comfort and energy costs in a residential nZEB, Buildings (2017) 7.
[19] T. Weiß, A.M. Fulterer, A. Knotzer, Energy flexibility of domestic thermal loads – a building typology approach of the residential building stock in Austria, Adv. Build. Energy Res. (2017) 1–16, https://doi.org/10.1080/17512549.2017.1420606.
[20] T. Cheung, G. Brager, T. Parkinson, P. Li, S. Schiavon, Analysis of the accuracy on PMV – PPD model using the ASHRAE global thermal comfort database II, Build. Environ. (2019), https://doi.org/10.1016/j.buildenv.2019.01.055.
[21] B. Koelblen, A. Psikuta, A. Bogdan, S. Annaheim, R.M. Rossi, Thermal sensation models: validation and sensitivity towards thermo-physiological parameters, Build. Environ. 130 (2018) 200–211, https://doi.org/10.1016/j.buildenv.2017.12.020.
[22] K. Katić, R. Li, W. Zeiler, Thermophysiological models and their applications: a review, Build. Environ. 106 (2016) 286–300, https://doi.org/10.1016/j.buildenv.2016.06.031.
[23] Y. Takahashi, A. Nomoto, S. Yoda, R. Hisayama, M. Ogata, Y. Ozeki, S. Tanabe, Thermoregulation model JOS-3 with new open source code, Energy Build. 231 (2021) 110575, https://doi.org/10.1016/j.enbuild.2020.110575, 110575.
[24] D. Fiala, K.J. Lomas, M. Stohrer, Computer prediction of human thermoregulatory and temperature responses to a wide range of environmental conditions, Int. J. Biometeorol. 45 (2001) 143–159, https://doi.org/10.1007/s004840100099.
[25] C. Huizenga, Z. Hui, E. Arens, A model of human physiology and comfort for assessing complex thermal environments, Build. Environ. 36 (2001) 691–699, https://doi.org/10.1016/S0360-1323(00)00061-5.
[26] B.R.M. Kingma, L. Schellen, A.J.H. Frijns, W.D. van Marken Lichtenbelt, Thermal sensation: a mathematical model based on neurophysiology, Indoor Air 22 (2012) 253–262, https://doi.org/10.1111/j.1600-0668.2011.00758.x.
[27] A.P. Gagge, J.A.J. Stolwijk, Y. Nishi, Effective temperature scale based on a simple model of human physiological regulatory response, Build. Eng. 77 (1971) 247–263.
[28] ASHRAE, ANSI/ASHRAE Standard 55-2020 - Thermal Environmental Conditions for Human Occupancy, 2020.
[29] D. Fiala, K.J. Lomas, M. Stohrer, First principles modeling of thermal sensation responses in steady-state and transient conditions, 179–186, https://doi.org/10.1590/S1517-83822008000200021, 2003.
[30] S. Takada, S. Matsumoto, T. Matsushita, Prediction of whole-body thermal sensation in the non-steady state based on skin temperature, Build. Environ. 68 (2013) 123–133, https://doi.org/10.1016/j.buildenv.2013.06.004.
[31] C.L. Tan, Z.A. Knight, Regulation of body temperature by the nervous system, Neuron 98 (2018) 31–48, https://doi.org/10.1016/j.neuron.2018.02.022.
[32] R. Xiao, X.Z.S. Xu, Temperature sensation: from molecular thermosensors to neural circuits and coding principles, Annu. Rev. Physiol. 83 (2021) 205–230, https://doi.org/10.1146/annurev-physiol-031220-095215.

[33] G.D. Mower, Perceived intensity of peripheral thermal stimuli is independent of internal body temperature, J. Comp. Physiol. Psychol. 90 (1976) 1152–1155, https://doi.org/10.1037/h0077284.

[34] M. Cabanac, P. Serres, Peripheral heat as a reward for heart rate response in the curarized rat, J. Comp. Physiol. Psychol. 90 (1976) 435–441, https://doi.org/10.1037/h0077213.

[35] A.P. Gagge, J.A.J. Stolwijk, J.D. Hardy, Comfort and thermal sensations and associated physiological responses at various ambient temperatures, Environ. Res. 1 (1967) 1–20, https://doi.org/10.1016/0013-9351(67)90002-3.

[36] R.J. de Dear, J.W. Ring, P.O. Fanger, Thermal sensations resulting from sudden ambient temperature changes, Indoor Air 3 (1993) 181–192, https://doi.org/10.1111/j.1600-0668.1993.t01-1-00004.x.

[37] H. Hensel, Functional and structural basis of thermoreception, 105–118, https://doi.org/10.1016/S0079-6123(08)64343-5, 1976.

[38] H. Hensel, Thermoreception and temperature regulation, Monogr. Physiol. Soc. 38 (1981) 1–321.

[39] M. Cabanac, Sensory pleasure, Q. Rev. Biol. 54 (1979) 1–29, https://doi.org/10.1086/410981.

[40] T. Parkinson, R. De Dear, Thermal pleasure in built environments: spatial alliesthesia from contact heating, Build. Res. Inf. 44 (2016) 248–262, https://doi.org/10.1080/09613218.2015.1082334.

[41] T. Parkinson, R. De Dear, C. Candido, Thermal pleasure in built environments: alliesthesia in different thermoregulatory zones, Build. Res. Inf. 44 (2016) 20–33, https://doi.org/10.1080/09613218.2015.1059653.

[42] T. Parkinson, R. de Dear, Thermal pleasure in built environments: spatial alliesthesia from air movement, Build. Res. Inf. 45 (2017) 320–335, https://doi.org/10.1080/09613218.2016.1140932.

[43] M. Vellei, R. de Dear, J. Le Dreau, J. Nicolle, Thermal Alliesthesia under Whole-Body Step-Change Transients, 2023. Tokyo, Japan.

[44] M. Vellei, R. de Dear, J. Le Dreau, J. Nicolle, M. Rendu, M. Doya, Thermal Alliesthesia under Whole-Body Cyclical Conditions, Aachen, Germany, 2023.

[45] A.D. Flouris, Z.J. Schlader, Human behavioral thermoregulation during exercise in the heat, Scand. J. Med. Sci. Sports 25 (2015) 52–64, https://doi.org/10.1111/sms.12349.

[46] Y. Ouzzahra, G. Havenith, B. Redortier, Regional distribution of thermal sensitivity to cold at rest and during mild exercise in males, J. Therm. Biol. 37 (2012) 517–523, https://doi.org/10.1016/j.jtherbio.2012.06.003.

[47] N. Gerrett, Y. Ouzzahra, S. Coleby, S. Hobbs, B. Redortier, T. Voelcker, G. Havenith, Thermal sensitivity to warmth during rest and exercise: a sex comparison, Eur. J. Appl. Physiol. 114 (2014) 1451–1462, https://doi.org/10.1007/s00421-014-2875-0.

[48] N. Gerrett, Y. Ouzzahra, B. Redortier, T. Voelcker, G. Havenith, Female thermal sensitivity to hot and cold during rest and exercise, Physiol. Behav. 152 (2015) 11–19, https://doi.org/10.1016/j.physbeh.2015.08.032.

[49] M. Vellei, G. Chinazzo, K.-M. Zitting, J. Hubbard, Human thermal perception and time of day: a review, Temperature (2021) 1–22, https://doi.org/10.1080/23328940.2021.1976004.

[50] D.R. Kenshalo, Changes in the cool threshold associated with phases of the menstrual cycle, J. Appl. Physiol. 21 (1966) 1031–1039, https://doi.org/10.1152/jappl.1966.21.3.1031.

[51] D.J. Cunningham, M. Cabanac, Evidence form behavioral thermoregulatory responses of a shift in setpoint temperature related to the menstrual cycle, J. Physiol. (Paris) 63 (1971) 236–238.

[52] F.C. Baker, F. Siboza, A. Fuller, Temperature regulation in women: effects of the menstrual cycle, Temperature 7 (2020) 226–262, https://doi.org/10.1080/23328940.2020.1735927.

[53] J.A. Boulant, Role of the preoptic-anterior hypothalamus in thermoregulation and fever, Clin. Infect. Dis. 31 (2000) S157–S161, https://doi.org/10.1086/317521.

[54] A.P. Gagge, A.P. Fobelets, L.G. Berglund, A standard predictive index of human response to the thermal environment, Build. Eng. 92 (1986) 709–731.

[55] T. Doherty, E. Arens, Evaluation of the physiological bases of thermal comfort models, Build. Eng. 94 (1988) 1371–1385.

[56] R.A. Haslam, An Evaluation of Models of Human Response to Hot and Cold Environments, 1989.

[57] Ankit Rohatgi, WebPlotDigitizer. https://automeris.io/WebPlotDigitizer, 2022.

[58] F.H. Rohles, Thermal sensations of sedentary man in moderate temperatures, Hum. Factors: J.Hum. Factors Ergon. Soc 13 (1971) 553–560, https://doi.org/10.1177/001872087101300606.

[59] P.E. McNall Jr., F.H. Rohles, R.G. Nevins, W. Springer, Thermal comfort (thermally neutral) conditions for three levels of activity, Build. Eng. 73 (1967) 1–14.

[60] F. Tartarini, S. Schiavon, pythermalcomfort: a Python package for thermal comfort research, SoftwareX 12 (2020) 100578, https://doi.org/10.1016/j.softx.2020.100578, 100578.

[61] M. Fountain, C. Huizenga, A Thermal Sensation Model for Use by the Engineering Profession, 1995.

[62] ASHRAE, ASHRAE Handbook—Fundamentals, 2021, 2021.

[63] W. Ji, M. Luo, B. Cao, Y. Zhu, Y. Geng, B. Lin, A new method to study human metabolic rate changes and thermal comfort in physical exercise by CO2 measurement in an airtight chamber, Energy Build. 177 (2018) 402–412, https://doi.org/10.1016/j.enbuild.2018.08.018.

[64] X. Jia, S. Li, Y. Zhu, W. Ji, B. Cao, Transient thermal comfort and physiological responses following a step change in activity status under summer indoor environments, Energy Build. 285 (2023), https://doi.org/10.1016/j.enbuild.2023.112918.

[65] Y. Lin, H. Jin, Y. Jin, J. Kang, Experimental study on the effects of exercise intensity and thermal environment on thermal responses, Build. Environ. 232 (2023) 110067, https://doi.org/10.1016/j.buildenv.2023.110067, 110067.

[66] A. Valenza, A. Bianco, D. Filingeri, Thermosensory mapping of skin wetness sensitivity across the body of young males and females at rest and following maximal incremental running, J. Physiol. 597 (2019) 3315–3332, https://doi.org/10.1113/JP277928.

[67] A. Gómez Del Campo, F. Viana, Detecting warm temperatures is a cool kind of thing, Neuron 106 (2020) 712–714, https://doi.org/10.1016/j.neuron.2020.05.009.

[68] R. Paricio-Montesinos, F. Schwaller, A. Udhayachandran, F. Rau, J. Walcher, R. Evangelista, J. Vriens, T. Voets, J.F.A. Poulet, G.R. Lewin, The sensory coding of warm perception, Neuron 106 (2020) 830, https://doi.org/10.1016/j.neuron.2020.02.035, 841.e3.

[69] M.A. Humphreys, J. Fergus Nicol, The validity of ISO-PMV for predicting comfort votes in every-day thermal environments, Energy Build. 34 (2002) 667–684, https://doi.org/10.1016/S0378-7788(02)00018-X.

[70] S. Karjalainen, Thermal comfort and gender: a literature review, Indoor Air 22 (2012) 96–109, https://doi.org/10.1111/j.1600-0668.2011.00747.x.

[71] M. Schweiker, G.M. Huebner, B.R.M. Kingma, R. Kramer, H. Pallubinsky, Drivers of diversity in human thermal perception – a review for holistic comfort models, Temperature 5 (2018) 308–342, https://doi.org/10.1080/23328940.2018.1534490.

[72] Z. Wang, R. de Dear, M. Luo, B. Lin, Y. He, A. Ghahramani, Y. Zhu, Individual difference in thermal comfort: a literature review, Build. Environ. 138 (2018) 181–193, https://doi.org/10.1016/j.buildenv.2018.04.040.

[73] H. Zhang, C. Huizenga, E. Arens, T. Yu, Considering individual physiological differences in a human thermal model, J. Therm. Biol. 26 (2001) 401–408, https://doi.org/10.1016/S0306-4565(01)00051-1.

[74] M. Vellei, R. de Dear, J. Le Dreau, J. Nicolle, M. Rendu, M. Abadie, G. Michaux, M. Doya, Dynamic thermal perception under whole-body cyclical conditions: thermal overshoot and thermal habituation, Build. Environ. 226 (2022) 109–677, https://doi.org/10.1016/j.buildenv.2022.109677.

[75] J.F. Nicol, M.A. Humphreys, Adaptive thermal comfort and sustainable thermal standards for buildings, Energy Build. 34 (2002) 563–572, https://doi.org/10.1016/S0378-7788(02)00006-3.

[76] N.A.S. Taylor, Human heat adaptation, Compr. Physiol. (2014), https://doi.org/10.1002/cphy.c130022.

[77] H.A.M. Daanen, W.D. Van Marken Lichtenbelt, Human whole body cold adaptation, Temperature (2016), https://doi.org/10.1080/23328940.2015.1135688.

[78] W. Ji, B. Cao, M. Luo, Y. Zhu, Influence of short-term thermal experience on thermal comfort evaluations: a climate chamber experiment, Build. Environ. 114 (2017) 246–256, https://doi.org/10.1016/j.buildenv.2016.12.021.

[79] Z. Zhang, Y. Zhang, E. Ding, Acceptable temperature steps for transitional spaces in the hot-humid area of China, Build. Environ. 121 (2017) 190–199, https://doi.org/10.1016/j.buildenv.2017.05.026.

[80] Y. Zhai, S. Zhao, L. Yang, N. Wei, Q. Xu, H. Zhang, E. Arens, Transient human thermophysiological and comfort responses indoors after simulated summer commutes, Build. Environ. 157 (2019) 257–267, https://doi.org/10.1016/j.buildenv.2019.04.023.

[81] T. Parkinson, H. Zhang, E. Arens, Y. He, R. de Dear, J. Elson, A. Parkinson, C. Maranville, A. Wang, Predicting thermal pleasure experienced in dynamic environments from simulated cutaneous thermoreceptor activity, Indoor Air (2021), https://doi.org/10.1111/ina.12859 ina.12859-ina.12859.